Electrochemical Investigation of Melittin Reconstituted into a Mercury-Supported Lipid Bilayer

ARTICLE *in* LANGMUIR · JULY 2006

Impact Factor: 4.46 · DOI: 10.1021/la060681x · Source: PubMed

Electrochemical Investigation of Melittin Reconstituted into a Mercury-Supported Lipid Bilayer

Lucia Becucci,[†] Reyes Romero León,[†,§] Maria Rosa Moncelli,[†] Paolo Rovero,[‡] and Rolando Guidelli*[,†]

Department of Chemistry, Florence University, Via della Lastruccia 3, 50019 Sesto Fiorentino, Firenze, Italy, and Laboratory of Peptides and Proteins Chemistry and Biology, Department of Pharmaceutical Sciences, Florence University, Via della Lastruccia 5, 50019 Sesto Fiorentino, Firenze, Italy

Received March 13, 2006. In Final Form: May 13, 2006

The channel-forming peptide melittin was incorporated into a biomimetic membrane consisting of a mercury electrode coated with a thiolipid monolayer, with a lipid monolayer self-assembled on top of it. The thiolipid consisted of a hydrophilic tetraethyleneoxy chain terminated at one end with a disulfide group, for anchoring to the mercury surface, and covalently linked at the other end to two diphytanyl chains, which formed a lipid bilayer with the overhanging lipid monolayer. The conductance of the lipid bilayer in contact with aqueous 0.1 M KCl was measured by electrochemical impedance spectroscopy over a frequency range from 1×10^{-2} to 1×10^{5} Hz and a potential range of 0.7 V for different compositions of the outer lipid monolayer. The conductance increases abruptly above the background level at sufficiently negative applied potentials, attaining a maximum value that increases with the composition of the outer monolayer in the order PC/chol (60:40) < PC < PC/SM/chol (59:15:26) < PS, with PC = phosphatidylcholine, chol = cholesterol, SM = sphingomyelin, and PS = phosphatidylserine. The higher the maximum conductance, the less negative the applied potential at which it is attained. This behavior is also discussed using a model of the electrified interphase.

Introduction

The polypeptide melittin is the major component of the venom of the honey bee. The peptide carries five positive charges from lysine and arginine residues. From its aqueous solutions, melittin binds spontaneously to biomembranes and bilayer lipid membranes (BLMs). At low concentrations, it induces voltage-gated channels in BLMs, whereas at concentrations higher than 1.2 μg/mL it causes their disruption.[1] When bound to lipid bilayers, melittin adopts a highly α-helical conformation, with most hydrophobic residues on one side and most hydrophilic residues on the opposite side of the helix long axis. At zero transmembrane potential, these amphipathic helices accumulate on the surface of the membrane, parallel to the plane of the bilayer. As the transmembrane potential is made negative on the opposite side of the membrane with respect to melittin, the helices form membrane-spanning aggregates that induce pore conductance.

The lipid bilayer environment has been found to affect the lytic activity of melittin, as measured by the loss of fluorescent dyes from vesicles. Thus, lipids with negatively charged headgroups and cholesterol (chol) have been reported to inhibit the lytic activity of melittin.[2] Matsuzaki et al.[3] reported that higher doses of melittin were required to permeabilize phosphatidylserine/sphingomyelin compared to the doses required for pure phosphatidylcholine vesicles. In contrast, sphingomyelin was reported to stimulate melittin pore formation in electrically neutral bilayers.[4] The alkyl chains of the lipids have also been reported to modulate the membrane-disruptive action of melittin.[5] Different views exist on the architecture of the pores induced by melittin. According to the barrel stave model, melittin molecules span a nearly flat bilayer and aggregate to line an aqueous channel.[6] However, according to the toroidal pore model, the lipid bilayer sharply bends so that the lipid headgroups form part of the lining of the pore.[2k,7]

The present work reports an investigation of the behavior of melittin incorporated into a mercury-supported biomimetic membrane. This was obtained by tethering to a mercury electrode a thiolipid consisting of a tetraethyleneoxy (TEO) hydrophilic chain terminated at one end with a disulfide group, for anchoring to the mercury surface, and covalently linked at the other end to two diphytanyl chains mimicking the hydrocarbon tails of a phospholipid. By self-assembling a lipid monolayer on top of the thiolipid monolayer, a lipid bilayer was obtained that was interposed between the TEO hydrophilic "spacer" and a 0.1 M KCl aqueous electrolyte.[8] The conductance of the resulting tethered bilayer lipid membrane (tBLM) induced by melittin was monitored as a function of the applied potential by using

* Corresponding author. E-mail: rolando.guidelli@unifi.it. Tel: +39-055-4573097.

† Department of Chemistry, Florence University.

‡ Department of Pharmaceutical Sciences, Florence University.

§ Present address: Department of Physical Chemistry, Sevilla University, Spain.

(1) (a) Pawlak, M.; Stankowski, S.; Schwarz, G. *Biochim. Biophys. Acta* **1991**, *1062*, 94−102. (b) Tosteson, M. Y.; Tosteson, D. C. *Biophys. J.* **1981**, *36*, 109−116.

(2) (a) Portlock, S. H.; Clague, M. J.; Cherry, R. J. *Biochim. Biophys. Acta* **1990**, *1030*, 1−10. (b) Monette, M.; Van Calsteren, M.-R.; Lafleur, M. *Biochim. Biophys. Acta* **1993**, *1149*, 319−328. (c) Ohki, S.; Marcus, E.; Sukumaran, D. H.; Arnold, K. *Biochim. Biophys. Acta* **1994**, *1194*, 223−232. (d) Monette, M.; Lafleur, M. *Biophys. J.* **1995**, *68*, 187−195. (e) Pott, T.; Dufourc, E. J. *Biophys. J.* **1995**, *68*, 965−977. (f) Benachir, T.; Lafleur, M. *Biochim. Biophys. Acta* **1995**, *1235*, 452−460. (g) Hincha, D. K.; Crowe, J. H. *Biochim. Biophys. Acta* **1996**, *1284*, 162−170. (h) Rex, S.; Bian, J.; Silvius, J.; Lafleur, M. *Biochim. Biophys. Acta* **2002**, *1558*, 211−221. (i) Raghuraman, H.; Chattopadhyay, A. *Biophys. J.* **2004a**, *87*, 2419−2432. (j) Allende, D.; McIntosh, T. J. *Biochemistry* **2003**, *42*, 1101−1108. (k) Allende, D.; Simon, S. A.; McIntosh, T. J. *Biophys. J.* **2005**, *88*, 1828−1837.

(3) Matsuzaki, K.; Sugishita, K.; Fuji, N.; Miyajima, K. *Biochemistry* **1995**, *34*, 3423−3429.

(4) Gómara, M. J.; Nir, S.; Nieva, L. L. *Biochim. Biophys. Acta* **2003**, *1612*, 83−89.

(5) (a) Rex, S. *Biophys. Chem.* **1996**, *58*, 75−85. (b) Raghuraman. H.; Chattopadhyay, A. *Biochim. Biophys. Acta* **2004b**, *1665*, 29−39.

(6) (a) Ladokhin, A. S.; White, S. H. *Biochim. Biophys. Acta* **2001**, *1514*, 253−260. (b) Rex, S.; Schwarz, G. *Biochemistry* **1998**, *37*, 2336−2345.

(7) Yang, L.; Harroun, T. A.; Weiss, T. M.; Ding, L.; Huang, H. W. *Biophys. J.* **2001**, *81*, 1475−1485.

10.1021/la060681x CCC: $33.50
Published on Web 06/17/2006

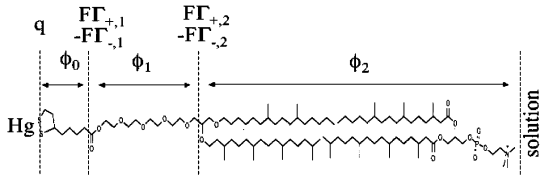

Figure 1. Primary structure of the tBLM, with the various substructural elements and the assumed distribution of charges.

electrochemical impedance spectroscopy (EIS). The effect exerted by the composition of the lipid monolayer self-assembled on top of the thiolipid upon the melittin-induced conductance was investigated and discussed.

Materials and Methods

The water used was obtained from water produced by an inverted osmosis unit upon distilling it once and then distilling the water so obtained from alkaline permanganate. Merck suprapur KCl was baked at 500 °C before use to remove any organic impurities. Diphytanoylphosphatidylcholine (PC) and diphytanoylphosphatidylserine (PS) were purchased in chloroform solution from Avanti Polar Lipids (Birmingham, AL). The transition temperatures of PC, PS, and Sphingomyelin (SM) were obtained from Lipid Products (Surrey, U.K.). Cholesterol (chol) was purchased from Sigma and used without further purification. The 2,3,di-*O*-phytanyl-*sn*-glycerol-1-tetraethylene-glycol-D,L-α lipoic acid ester lipid (DPTL) was obtained from the Max Plank Institute for Polymer Research in Mainz.[9] It consists of a TEO chain covalently linked to a lipoic acid residue for anchoring to the metal at one end and bound via ether linkages to two phytanyl chains, 16 carbon atoms long, at the other end (Figure 1). The transition temperatures of PC, PS, and DPTL from the gel to the liquid-crystalline state are not higher than −40 °C.

Melittin was synthesized manually, in a stepwise fashion, by the solid-phase 9-fluorenylmethoxy-carbonyl (Fmoc)/9-fluorenylmethoxy-carbonyl method. Protected amino acids were added stepwise to TentaGel S RAM resin (capacity: 0.24 mmol/g); each coupling reaction was accomplished using a 5-fold amino acid molar excess with equimolar *O*-(benzotriazol-1-yl)-1,1,3,3-tetramethyluronium hexafluorophosphate/1-hydroxybenzotriazole in the presence of *N*-methylmorpholine (6-fold excess) for 40 min. The N^{α}-Fmoc protecting groups were removed after each coupling cycle by treatment with 20% piperidine in dimethylformamide for 10 min. The peptide was released from the resin with trifluoroacetic acid (TFA)/H_2O/tri-isopropyl silane (90:5:5 v/v/v) for 90 min. The resin was removed by filtration, and the crude peptide was recovered by precipitation with cold ethyl ether to give a white powder. Finally, the crude peptide was dissolved in CH_3COOH/H_2O (1:50 v/v) and lyophilized. Peptide purification was performed by semipreparative high-performance liquid chromatography (HPLC) on a Vydac C18 218TP column (10 × 250 mm^2, 10 μ 300 Å pore size) using a linear gradient of CH_3CN in water containing 0.1% TFA. The final product was obtained by lyophilization of the appropriate fractions after removal of the CH_3CN by rotary evaporation. Analytical reverse-phase HPLC (Phenomenex-Jupiter C18 column 250 × 4.6 mm^2, 5 μ 300 Å pore size, linear gradient 5−71% in 22 min of CH_3CN in water containing 0.1% TFA at a flow rate of 1 mL/min; UV detection: 210 nm, Rt: 18.0 min) indicated >97% purity. Molecular mass was determined on a Finningan LCQ-Deca ion trap instrument equipped with an electrospray source (MH^+ found, 2847.2; calcd, 2847.5). The other chemicals and solvents were commercially available and used as received.

SM and chol stock solutions were prepared by dissolving these lipids in chloroform. PC and PS solutions were prepared by diluting proper amounts of stock solutions of these phospholipids with pentane. Lipid mixtures were obtained by diluting proper amounts of each lipid stock solution with pentane to obtain the following compositions: PC/chol (60:40) and PC/SM/chol (59:15:26). Solutions of 0.2 mg/mL DPTL in ethanol were prepared from a 2 mg/mL solution of DPTL in ethanol. Stock solutions of this thiolipid were stored at −18 °C. Stock solutions of 0.2 mg/mL melittin in water were stored at +4 °C.

All measurements were carried out in aqueous 0.1 M KCl. The pH of this unbuffered solution ranged from 5.8 to 6.0. Differences with respect to solutions buffered at pH 7 with a 5×10^{-3} M phosphate buffer, under otherwise identical conditions, were found to lie within the limits of experimental error. Use was made of a homemade hanging mercury drop electrode (HMDE), described elsewhere.[10] A homemade glass capillary with a finely tapered tip, about 1 mm in outer diameter, was employed. The capillary and mercury reservoir were thermostated at 25 ± 0.1 °C in a water-jacketed box to avoid any changes in drop area due to a change in temperature. One glass electrolysis cell containing the aqueous solution and a small glass vessel containing the ethanol solution of the thiolipid were placed on a movable support inside the box.[11] The HMDE and the support were moved vertically and horizontally by means of two oleodynamic systems that ensured the complete absence of vibrations. ac voltammetry and impedance spectroscopy measurements were carried out with an Autolab instrument (Echo Chemie) supplied with the FRA2 module for impedance measurements, a SCAN-GEN scan generator, and GPES 4.9005 Beta software. Potentials were measured versus a Ag|AgCl electrode immersed in the 0.1 M KCl working solution. Impedance spectra were recorded by scanning the bias potential in 25 mV steps in the chosen direction and by varying the frequency of a 10 mV peak-to-peak ac signal over the range from 1×10^{-2} to 1×10^{5} Hz at each bias potential.

Monolayers of DPTL were self-assembled on the HMDE by keeping the mercury drop immersed in the small vessel containing the thiolipid solution for 20 min. In the meantime, a lipid solution in pentane was spread on the surface of the aqueous solution in the glass cell in an amount corresponding to five to six lipid monolayers, and the pentane was allowed to evaporate. Using the oleodynamic system, the DPTL-coated HMDE was then extracted from the vessel, washed with ethanol to remove the excess adsorbed thiolipid, and kept in a N_2 atmosphere for the time strictly necessary to allow the solvent to evaporate. Immediately afterward, the electrolysis cell containing the aqueous solution on whose surface the lipid film had been previously spread was brought below the HMDE, and the latter was lowered so as to immerse it into the aqueous solution across the lipid film; this procedure causes a lipid monolayer to self-assemble on top of the DPTL monolayer, giving rise to a lipid bilayer interposed between the hydrophilic moiety of the thiolipid and the aqueous solution. The applied potential was then repeatedly scanned over a potential range from −0.200 to −1.200 V while continuously monitoring the curve of the quadrature component, Y'', of the electrode admittance at 75 Hz against the applied potential, E, using ac voltammetry until a stable Y'' versus E curve was attained. The minimum differential capacity of the resulting (DPTL/lipid)-coated mercury ranged from 0.55 to 0.65 μF cm^{-2} and was therefore close to the capacity, ∼0.8 μF cm^{-2}, of a solvent-free black lipid membrane.[12] Melittin was incorporated in this tBLM by simply adding its stock solution to the electrolysis cell in an amount corresponding to 1.4×10^{-7} M. The solution was then stirred for 5 min while keeping the electrode at an applied potential of −0.500 V.

(8) (a) Moncelli, M. R.; Becucci, L.; Schiller, S. M. *Bioelectrochemistry* **2004**, *63*, 161−167. (b) Becucci, L.; Moncelli, M. R.; Guidelli, R. *J. Am. Chem. Soc.* **2005**, *127*, 13316−13323. (c) Becucci, L.; Moncelli, M. R.; Guidelli, R. *Langmuir* **2006**, *22*, 1341−1346.

(9) (a) Schiller, S. M.; Naumann, R.; Lovejoy, K.; Kunz, H.; Knoll, W. *Angew. Chem., Int. Ed.* **2003**, *42*, 208−211. (b) Naumann, R.; Schiller, S. M.; Giess, F.; Grohe, B.; Hartman, K. B.; Karcher, I.; Koper, I.; Lubben, J.; Vasilev, K.; Knoll, W. *Langmuir* **2003**, *19*, 5435−5443.

(10) Moncelli, M. R.; Becucci, L. *J. Electroanal. Chem.* **1997**, *433*, 91−96.

(11) Tadini Buoninsegni, F.; Herrero, R.; Moncelli, M. R. *J. Electroanal. Chem.* **1998**, *452*, 33−42.

(12) Montal, M.; Mueller, P. *Proc. Natl. Acad. Sci. U.S.A.* **1972**, *69*, 3561−3566.

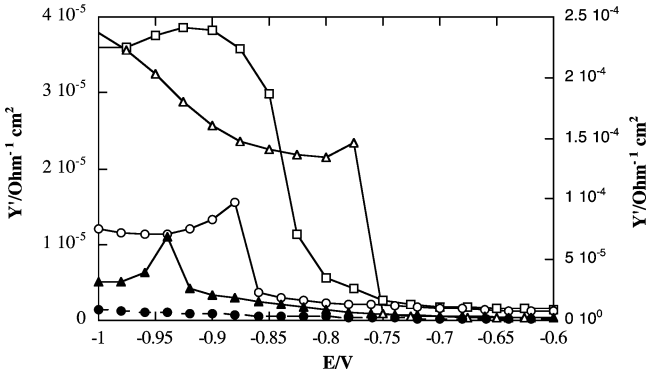

Figure 2. Plot of the in-phase component Y' of the electrode admittance at 10 Hz against E for tBLMs of different outer-monolayer composition: PC/chol (▲), PC (○), PC/SM/chol (□), PS (△) upon incorporation of melittin from its 1.4×10^{-7} M solution in aqueous 0.1 M KCl. The Y' vs E plot for a tBLM with PC outer-monolayer composition in the absence of melittin is dashed and denoted by solid circles. The left-hand vertical axis refers to PC/chol, PC, and PC/SM/chol, and the right-hand one, to PS.

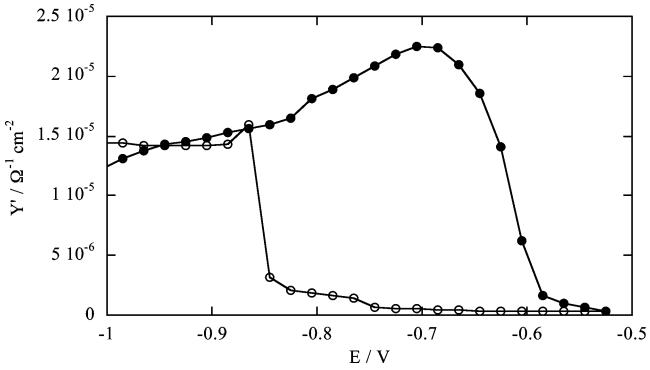

Figure 3. Plot of the in-phase component Y' of the electrode admittance at 10 Hz against E for a DPTL/PC tBLM, upon incorporation of melittin from its 1.4×10^{-7} M solution in aqueous 0.1 M KCl. Y' was first recorded from −0.500 to −1.00 V (○) and then backward (●).

Results

Impedance spectra of tBLMs incorporating melittin were recorded in aqueous 0.1 M KCl over a potential range from −0.3 to −1.00 V and over a frequency range from 1×10^{-2} to 1×10^5 Hz for different compositions of the lipid monolayer in direct contact with the aqueous solution. The presence of melittin increases both the in-phase and the quadrature components of the tBLM admittance. Figure 2 shows plots of the in-phase component, Y', of the tBLM admittance against the applied potential, E, after the incorporation of melittin from an aqueous solution of 0.1 M KCl and 1.4×10^{-7} M melittin for different compositions of the outer lipid monolayer and at a constant frequency $\nu = 10$ Hz. It is apparent that Y', which is a rough measure of the conductance of the tBLM, increases in the order DPTL/(PC/chol) < DPTL/PC < DPTL/(PC/SM/chol) < DPTL/PS; this increase is accompanied by a shift in the steep rising section of the Y' versus E plot toward less-negative E values. It should be noted that the tBLM is stable for an indefinitely long time over the potential range covered in Figure 2 for all compositions of the outer lipid monolayer. Moreover, its conductance in the absence of melittin is much lower than that observed in its presence, as shown by the dashed curve in this Figure, which refers to the DPTL/PC composition; analogous curves obtained for the other outer monolayer compositions are indistinguishable from this dashed curve on the time scale of Figure 2.

If Y' is recorded against E by scanning the potential from −0.500 to −1.00 V and then immediately afterward in the opposite direction, notable hysteresis is observed. This behavior is shown in Figure 3 for the DPTL/PC tBLM, but analogous behavior is also observed with the other compositions of the outer lipid monolayer. The magnitude of the hysteresis depends to some extent on the negative potential limit and on the rest time between the negative and positive potential scans. At any rate, in all cases, in the backward scan Y' drops to zero in the vicinity of −0.500 V.

To gain deeper insight into the behavior of the tBLM reconstituted with melittin, we must consider that the tBLM consists of substructural elements with different dielectric properties. In previous work,[8b] it was shown that the impedance spectra of the tBLM, both in the absence and in the presence of the ionophore valinomycin, can be satisfactorily fitted to an equivalent circuit consisting of four RC meshes in series. These are straightforwardly ascribed to the following dielectric slabs composing the tBLM and shown in Figure 1: the lipoic acid residue, the TEO moiety, the lipid bilayer, and the aqueous solution bathing the lipid bilayer. Roughly speaking, the conductance, $g_i = 1/R_i$, of the ith slab is a measure of the ac current flowing back and forth across this slab, whereas the corresponding capacity C_i, in parallel with R_i, measures the amount of charge that can be accumulated at the boundary that delimits the slab on its metal side. Whereas g_i primarily influences the higher-frequency range of the impedance spectrum, C_i influences the lower one. The R_iC_i product measures the "relaxation time" of the process taking place in the ith slab. Of the four slabs composing the tBLM, the lipoic acid residue, in direct contact with the mercury surface, is characterized by the highest resistance and behaves like a pure capacitive element.

Following the above approach, the impedance spectra of the tBLM incorporating melittin were fitted to an equivalent circuit consisting of a series of four RC meshes at each applied potential investigated. With this equivalent circuit, the best representation of the impedance spectrum at constant applied potential consists of plotting $\omega Z'$ against $\omega Z''$, where Z' and Z'' are the in-phase and quadrature components of the impedance, respectively, and ω is the angular frequency.[8b] In this type of plot, each R_iC_i mesh is represented by a semicircle; the diameter of the semicircle measures the reciprocal, $1/C_i$, of the capacity of the R_iC_i mesh, and the ω value at the maximum of the semicircle measures the reciprocal of its relaxation time, $\tau_i = R_iC_i$. Figure 4 shows two $\omega Z'$ versus $\omega Z''$ plots obtained with a DPTL/PC tBLM at −0.900 V (curve *a*) and with a DPTL/(PC/SM/chol) tBLM at −0.600 V (curve *b*), upon incorporating melittin. The frequency increases in the direction of increasing $\omega Z''$. The plot relative to the DPTL/PC tBLM (curve *a* in Figure 4) shows a depressed semicircular arc and, at higher frequencies, a small portion of a much larger semicircle. The latter is to be ascribed to the aqueous solution adjacent to the tBLM, whose capacity is approximately equal to 25 nF cm^{-2};[8b] it will not be considered further. Interestingly, the plot obtained with a DPTL/PC tBLM at −0.410 V upon incorporating valinomycin from its 1.5×10^{-7} M solution in aqueous 0.1 M KCl (dashed curve in Figure 4) differs from curve *a* by the fact that the depressed semicircular arc is replaced by three distinct partially fused semicircles that are ascribed, in order, to the lipoic acid residue, the TEO moiety, and the lipid bilayer when proceeding in the direction of increasing $\omega Z''$. Incidentally, in the pertinent literature, a depressed semicircular arc is often fitted to a particular circuit element called the constant phase element (CPE), whose use is justified when the relaxation time of the corresponding event is not single-valued but is

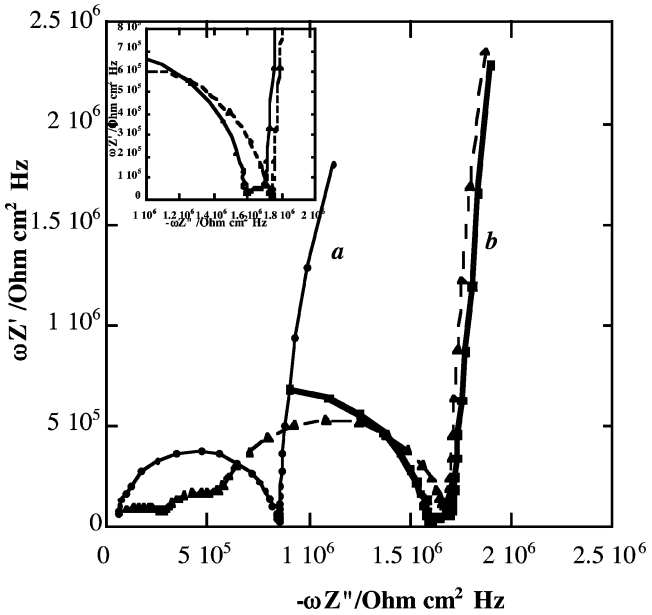

Figure 4. Plot of $\omega Z'$ vs $\omega Z''$ for a DPTL/PC tBLM at −0.900 V (a) and for a DPTL/(PC/SM/chol) tBLM at −0.600 V (b), upon incorporation of melittin from its 1.4×10^{-7} M solution in aqueous 0.1 M KCl. The dashed curve is a $\omega Z'$ vs $\omega Z''$ plot for a DPTL/PC tBLM at −0.410 V, upon incorporation of valinomycin from its 1.5×10^{-7} M solution in aqueous 0.1 M KCl. The inset shows a $\omega Z'$ vs $\omega Z''$ plot for a DPTL/(PC/SM/chol) tBLM at −0.600 V, both in the absence (- -) and in the presence (−) of 1.4×10^{-7} M melittin.

distributed continuously around a mean.[13] Alternatively, the arc may be depressed by a discrete number of relaxations whose time constants differ by less than 2 orders of magnitude. In the present case, comparing the impedance spectra of the tBLMs incorporating melittin and valinomycin strongly suggests that the depression of the arc of curve *a* in Figure 4 with respect to a semicircle is due to the overlapping of semicircles ascribable to the three above dielectric slabs composing the tBLM. The difference between curve *a* and the dashed curve in Figure 4 is due to 1.5×10^{-7} M valinomycin decreasing the resistance of the lipid bilayer much more than 1.4×10^{-7} M melittin. Consequently, the relaxation time of the lipid bilayer incorporating melittin is greater than that of the lipid bilayer incorporating valinomycin and lies in the vicinity of the relaxation times of the other substructural elements of the tBLM. This indicates that, under the present conditions, the number of channels formed by melittin molecules in the lipid bilayer is much less than the number of incorporated valinomycin molecules.

The contribution of the lipid-bilayer moiety to the depressed arc of curve *a* in Figure 4 is much greater than that of the other dielectric slabs. To confirm this statement, curve *a* was fitted to an equivalent circuit consisting of only two RC meshes in series, accounting exclusively for the depressed arc and for the small portion of the large arc due to the aqueous solution; the potential dependence of the resistance and capacity values ascribable to the depressed arc was found to be in semiquantitative agreement with that ascribable to the lipid-bilayer moiety in the fitting to four RC meshes in series. This also implies that the accuracy of the *R* and *C* values for the other two RC mashes, included to obtain a better fit to the depressed arc, is rather low. Consequently, only the potential dependence of the *R* and *C* circuit elements ascribable to the lipid-bilayer moiety in the fit to a series of four RC meshes will be reported in what follows. Identical considerations hold for the depressed arc obtained with the DPTL/(PC/chol), DPTL/PS and DPTL/(PC/SM/chol) tBLMs.

(13) Macdonald, J. R.; Johnson, W. B. *Impedance Spectroscopy*; Wiley and Sons: New York, 1987; p 1.

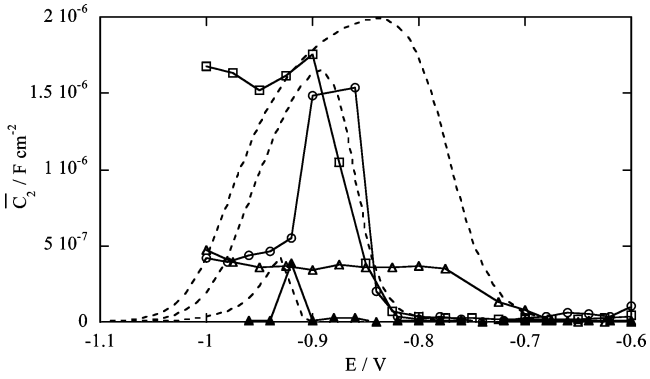

Figure 5. Plot of the capacity $\bar{C}_2$ of the lipid-bilayer moiety against *E* for tBLMs of different outer-monolayer composition: PC/chol (▲), PC (○), PC/SM/chol (□), and PS (△), upon incorporation of melittin from its 1.4×10^{-7} M solution in aqueous 0.1 M KCl. The three dashed curves were calculated from the model for $C_0 = 4\ \mu$F cm^{-2}, $C_1 = 7\ \mu$F cm^{-2}, $C_2 = 1\ \mu$F cm^{-2}, $\chi_1 = -0.250$ V, $a = 500$ V^{-1}, $\Delta = -0.030$ V, $K_{+,1} = K_{-,1} = 5 \times 10^{-3}$, $K_{+,2} = 3 \times 10^5$ cm^3 mol^{-1}, and (in order of increasing height) $K_{-,2} = 3 \times 10^4$, 5×10^5, and 1.5×10^6 cm^3 mol^{-1}.

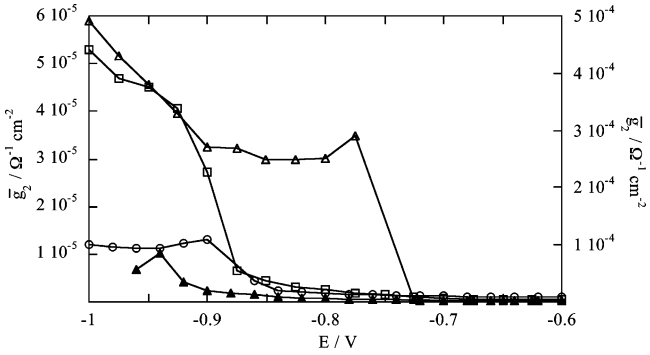

Figure 6. Plot of the conductance $\bar{g}_2$ of the lipid-bilayer moiety against *E* for tBLMs of different outer-monolayer composition: PC/chol (▲), PC (○), PC/SM/chol (□), and PS (△), upon incorporation of melittin from its 1.4×10^{-7} M solution in aqueous 0.1 M KCl. The left-hand vertical axis refers to PC/chol, PC, and PC/SM/chol, and the right-hand one, to PS.

Figures 5 and 6 show plots of the capacity, $\bar{C}_2$, and of the conductance, $\bar{g}_2$, of the lipid-bilayer moiety against *E* for the four different compositions of the outer lipid monolayer. Here and in the following text, overbarred quantities denote differences between the quantities measured in the presence of melittin and those measured in its absence on the same tBLM. In practice, such a subtraction has a detectable effect only on the capacity values. The $\bar{g}_2$ versus *E* plots are similar to the corresponding Y' versus *E* plots at 10 Hz in Figure 2, thus confirming that the conductance of the whole biomimetic membrane is mainly controlled by the lipid-bilayer moiety. The $\bar{C}_2$ values for the different lipid compositions have the same order of magnitude.

The $\omega Z'$ versus $\omega Z''$ plot at −0.600 V for the DPTL/(PC/SM/chol) tBLM incorporating melittin (curve b in Figure 4) differs from those for the other tBLMs of different lipid compositions by the presence of a small partially fused semicircle lying in the vicinity of $\omega Z'' = 1.6 \times 10^6\ \Omega$ cm^2 Hz at the back of the large semicircle due to the aqueous solution. No such semicircle is observed for the DPTL/(PC/SM/chol) tBLM at −0.600 V in the absence of melittin (inset of Figure 4). Interestingly, this small semicircle is observed only at potentials more positive than −0.800 V. It was accounted for by adding

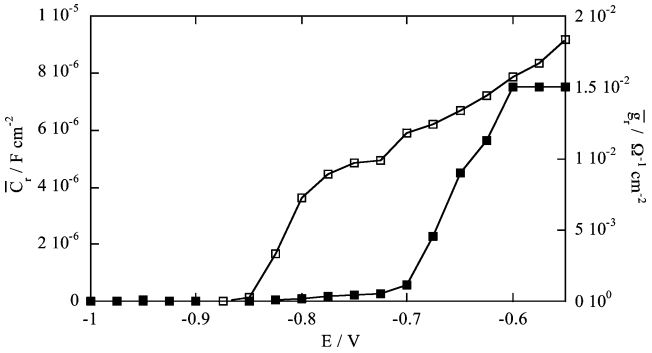

Figure 7. Plot of $\bar{C}_r$ (□) and $\bar{g}_r$ (■) against E for a DPTL/(PC/SM/chol) tBLM, upon incorporation of melittin from its 1.4×10^{-7} M solution in aqueous 0.1 M KCl.

another RC mesh to the equivalent circuit used for the fitting to curve b in Figure 4. The capacity and conductance of this additional RC mesh, denoted by $\bar{C}_r$ and $\bar{g}_r$, are plotted against E in Figure 7. In accordance with the short relaxation time and high characteristic frequency of this RC mesh, its conductance attains values that are more that 2 orders of magnitude higher than those of the corresponding lipid-bilayer moiety; both $\bar{C}_r$ and $\bar{g}_r$ decay practically to zero at potentials more negative than about −0.850 V, at which the conductance $\bar{g}_2$ of the lipid-bilayer moiety starts to increase because of the opening of the melittin channels.

Discussion

Even though K^+ and Cl^- ions are distributed in space across the tBLM, albeit nonhomogeneously, the ideal circuit elements used for the fitting represent ideal lumped-constant properties. A general approach outlined elsewhere[8b,c] relates these circuit elements to the substructural elements of the tBLM by assuming that the charges within the tBLM are located as follows (Figure 1): a free electronic charge density q on the surface of the mercury electrode, two charge densities $F\Gamma_{+,1}$ and $-F\Gamma_{-,1}$ at the boundary between the lipoic acid residue and the TEO moiety, and two charge densities $F\Gamma_{+,2}$ and $-F\Gamma_{-,2}$ at the boundary between the TEO moiety and the lipid bilayer. Here, $\Gamma_{+,1}$, $\Gamma_{+,2}$ and $\Gamma_{-,1}$, $\Gamma_{-,2}$ are surface concentrations of K^+ and Cl^- ions, respectively. The potential difference ϕ_t across the whole tBLM due to this charge distribution is expressed by the equation

$$\phi_t = \frac{q}{C_0} + \left[\frac{q + F(\Gamma_{+,1} - \Gamma_{-,1})}{C_1} + \chi_1\right] + \frac{q + F(\Gamma_{+,1} - \Gamma_{-,1} + \Gamma_{+,2} - \Gamma_{-,2})}{C_2} \equiv \phi_0 + \phi_1 + \phi_2 \quad (1)$$

Here, C_0, C_1, and C_2 are, in order, the "intrinsic" capacities of the lipoic acid residue, the TEO moiety, and the lipid bilayer, as measured in the absence of ionophores, and ϕ_0, ϕ_1, and ϕ_2 are the potential differences across these dielectric slabs. ϕ_1 includes the dipole potential, χ_1, of the TEO moiety, which was estimated to be about −0.250 V, negative toward the metal, on the basis of independent measurements.[8a] The extrathermodynamic absolute potential difference ϕ_t across the whole mercury|aqueous solution interphase is more positive than the potential E measured versus a SCE by about 0.250 V, which results from several pieces of experimental evidence. Therefore, ϕ_t can be directly related to the applied potential E.

The general approach ascribes each RC mesh to a substructural element of the tBLM. Roughly speaking, the conductance $\bar{g}_i$ of a given substructural element i is set equal to the rate of change with E of the current that flows back and forth along the element, and its capacity $\bar{C}_i$ is set equal to the rate of change with E of the charge that accumulates at the boundary of the element on its metal side. To this end, the currents, $j_{+,2}$ and $j_{-,2}$, that flow along the lipid-bilayer moiety and require the K^+ and Cl^- ions to surmount the corresponding potential energy barriers are expressed by Butler−Volmer-like equations.[8b,c] Under equilibrium conditions (i.e., for $j_{+,2} = j_{-,2} = 0$), these equations reduce to Langmuir isotherms, with potential-independent adsorption equilibrium constants, $K_{+,2}$ and $K_{-,2}$. Analogous expressions are used for the currents, $j_{+,1}$ and $j_{-,1}$, flowing along the TEO moiety. The resulting calculated capacities and conductances exclusively express the contributions to these quantities induced by the presence of ion channels, without the small contributions existing in their absence. For this reason, these calculated quantities must be compared with the overbarred quantities in Figures 5−7.

To predict the shape of the $\bar{C}_2$ versus E curves in Figure 5 on the basis of the model, the same parameters obtained in ref 8b for the tBLM in the absence of ionophores were employed, namely, the intrinsic capacities $C_0 = 4\ \mu F\ cm^{-2}$, $C_1 = 7\ \mu F\ cm^{-2}$, and $C_2 = 1\ \mu F\ cm^{-2}$ and the dipole potential $\chi_1 = -0.250$ V. Moreover, the equilibrium constants for the translocation of K^+ ions across the TEO moiety and across the lipid bilayer were set equal to $K_{+,1} = 5 \times 10^{-3}$ and $K_{+,2} = 3 \times 10^5\ cm^3\ mol^{-1}$, which were found to provide the best fit to the impedance spectra of a tBLM in contact with aqueous 0.1 M KCl and incorporating either the ion carrier valinomycin[8b] or the channel-forming protein OmpF porin.[8c] In the case of OmpF porin, which is permeated by both K^+ and Cl^-, the best fit of the impedance spectra to the equivalent circuit adopted herein was obtained by setting the equilibrium constant, $K_{-,1}$, for Cl^- translocation across the TEO moiety equal to that for the K^+ ion, and $K_{-,2} = 3\ cm^3\ mol^{-1}$. This very low $K_{-,2}$ value, as compared with the $K_{+,2}$ value, was justified both by the well-documented cation selectivity of OmpF porin and by K^+ ions interacting attractively with the ether oxygen atoms of the TEO moiety, as distinct from Cl^- ions. As opposed to OmpF porin, melittin exhibits anion selectivity.[14] The trend shown by the $\bar{C}_2$ versus E plots in Figure 5 was, therefore, justified qualitatively by the model upon ascribing to $K_{-,2}$ progressively increasing values as the lipid-bilayer conductance increases while keeping the equilibrium constant $K_{-,1}$ for Cl^- translocation across the TEO moiety unchanged and equal to that, 5×10^{-3}, for K^+ ions. The voltage-gated properties of melittin were simulated by multiplying $\bar{C}_2$ and $\bar{g}_2$ by the probability of melittin penetration into the lipid bilayer, with channel formation, as expressed by the well-known Boltzmann equation:

$$\frac{1}{1 + \exp[a(\phi_2 - \Delta)]} \quad (2)$$

A relatively satisfactory fit was obtained for $a = 500\ V^{-1}$ and $\Delta = -0.030$ V.

In accordance with experiment, the model predicts a progressive shift of the abrupt increase of both $\bar{C}_2$ and $\bar{g}_2$, which marks the opening of the melittin channels, toward less-negative applied potentials as $K_{-,2}$ increases with respect to $K_{+,2}$. This is due to the fact that, on account of the surface dipole potential of the TEO moiety, which is negative toward the mercury, potassium ions tend to accumulate on the metal side of the TEO moiety and chloride ions tend to accumulate on the solution side. At constant applied potential E, an increase in the accumulation of the latter anions causes a positive shift in the potential difference across the lipoic acid and TEO moieties and a concomitant negative

(14) Vogel, H.; Jahnig, F. *Biophys. J.* **1986**, *50*, 573−582.

shift in the potential difference across the lipid-bilayer moiety (i.e., the transmembrane potential). Therefore, the negative "threshold" value of the transmembrane potential at which the melittin channels start to open is attained at more positive applied potentials as $K_{-,2}$ increases with respect to $K_{+,2}$. The shape of the $\bar{g}_2$ versus E curves predicted by the model for the different lipid-monolayer compositions (data not shown) is similar to that predicted for the corresponding capacity $\bar{C}_2$ versus E curves.

In principle, the equilibrium constants for ion translocation across a lipid bilayer should not depend on the nature of the incorporated ionophore but only on the two phases separated by the bilayer. In practice, however, true equilibrium conditions are not attained even at the lowest frequencies adopted in the present ac measurements. Consequently, the differential capacity $\bar{C}_2$, which is estimated from the low-frequency range of the impedance spectrum, does not refer to true equilibrium conditions, and $K_{-,2}$ and $K_{+,2}$ should be regarded as pseudoequilibrium constants. The increase in $K_{-,2}$ in the order (PC/chol) < PC < PS is ascribable to a closer approach of Cl^- translocation across the lipid bilayer to true equilibrium conditions due to an increase in the unit conductance of each melittin channel and/or an increase in their number density as the composition of the outer lipid monolayer is varied. The slow approach to equilibrium conditions is also probably responsible for the hysteresis shown in Figure 3. As the applied potential is scanned back from −1.00 to −0.500 V, the slow release of potassium and chloride ions from the TEO ionic reservoir to the aqueous phase along the melittin channels ensures that the transmembrane potential is negative at the same applied potentials E at which it was positive during the preceding negative potential scan; this causes the melittin channels to remain open even at −0.60 V.

The model predicts an increase in the capacity of the lipid-bilayer moiety with an increase in $K_{-,2}$, as shown by the dashed curves in Figure 5. Even though, for the outer lipid monolayers investigated, PS is that on which the melittin-induced abrupt increase in $\bar{C}_2$ occurs at the most positive potential, in agreement with the highest $K_{-,2}$ value and with the highest conductance $\bar{g}_2$ (Figure 6), the maximum value attained by $\bar{C}_2$ is appreciably lower than that predicted by the model. This behavior can be tentatively ascribed to the negative charge on the PS polar heads, which tends to reduce the accumulation of translocated chloride ions at the boundary between the TEO moiety and the lipid bilayer by electrostatic repulsion, with a resulting decrease in $\bar{C}_2$.

The conductance of the DPTL/(PC/chol) bilayer being lower than that of the DPTL/PC bilayers agrees with the frequently reported decrease in the melittin-induced leakage of lipid vesicles upon increasing their chol content. The presence of chol in the lipid bilayer has a dual effect: it reduces the binding of the peptide to the bilayer [2b,i,j,4] and increases bilayer in-plane cohesive interactions. Thus, the introduction of chol into PC bilayers increases both the free energy of partitioning of melittin to the bilayer and the isothermal area compressibility modulus.[2k]

The highest melittin-induced conductance being attained with an outer PS monolayer (Figure 6) is in apparent contrast with the decreased level of melittin-induced leakage produced by the incorporation of PS in PC bilayers[2g,j] despite the concomitant increase in the level of melittin binding. The decrease in the lytic activity of melittin induced by negatively charged lipids has often been ascribed to these lipids anchoring melittin to the bilayer surface via electrostatic attractive interactions, thereby preventing melittin from penetrating deeply into the hydrocarbon tails of the bilayer.[2a,c,f,g,j] However, the extent of quenching of the intrinsic tryptophan fluorescence of melittin was found to be practically the same in PC and PC/PS (80:20) liposomes,[2g] thus indicating that the presence of PS does not reduce the insertion depth of the peptide into the bilayer. Moreover, Fourier transform infrared spectroscopy revealed specific interactions of melittin with the headgroups of PS and other negatively charged lipids.[2g] Even though electrochemical measurements provide no direct information on the molecular structure of the ion channel, in view of the last two findings we may speculate that melittin in PS-containing bilayers may form toroidal pores, as confirmed by different pieces of evidence gained with neutral bilayers.[2k,7] In a toroidal pore, the peptides are always associated with the lipid headgroups even when they are perpendicularly inserted into the lipid bilayer. In other words, the pore is lined with both the peptides and the lipid headgroups because of the sharp bending of the lipid bilayer around the pore. With this arrangement, the electrostatic attraction between the positively charged melittin molecules and the negatively charged PS headgroups does not prevent a perpendicular insertion of melittin in the lipid bilayer. It should also be noted that the melittin-induced lysis of lipid bilayers is measured by the release of bulky fluorescent molecules (e.g., calcein,[2f] carboxyfluorescein,[2g] and sulforhodamine B[2j]) from vesicles. Conversely, our conductance measurements involve the translocation across lipid bilayers of the small chloride and potassium ions. In this respect, our measurements should be compared with conductance measurements on BLMs bathed by aqueous solutions of monovalent inorganic ions. Thus, the minimal concentration of melittin required to produce a sustained increase in 1 M NaCl conductance was found to be equal to 0.02 μg/mL across a DOPS BLM and 0.4 μg/mL across a DOPC/DOPE (1:1) BLM,[15] in semiquantitative agreement with our results. The above discrepancy between leakage assays and conductance measurements may lead to speculation about the reason that bilayers of neutral lipids allow a much more pronounced melittin-induced leakage of bulky fluorescent dyes than bilayers of negatively charged lipids. In general, peptide insertion decreases the activation energy of pore formation by lowering the line tension along the edges of the pore. This effect is more pronounced with cationic peptides because of their mutual electrostatic repulsion, which tends to favor pore expansion.[16] In lipid bilayers containing negatively charged lipids, toroidal pores are lined by both the cationic peptides and the anionic headgroups; this reduces or eliminates the electrostatic repulsion among the pore-forming peptides and the resulting increase in pore expansion.

The appreciable increase in the conductance of the outer PC/chol monolayer upon addition of SM (Figures 2 and 6) is, to some extent, similar to the increase in the hemolytic activity of the earthworm hemolysin eiseniapore in vesicles containing both SM and chol.[17] It is tempting to hypothesize a preferential localization of melittin in chol/SM-rich microdomains (rafts) of the outer lipid monolayer, also because chol/SM plasma membrane rafts have been reported to act as concentration platforms for pore-forming toxins.[18] In addition, the Nef protein of HIV-1, whose terminal region resembles melittin, was reported to associate with membrane rafts for its activity.[19] Our results agree with leakage assays on POPC/SM/chol (1:1:1) large unilamellar vesicles (LUVs), which show an increase in the

(15) Feigin, A. M.; Teeter, J. H.; Brand, J. G. *Biochem. Biophys. Res. Commun*. **1995**, *211*, 312−317.
(16) Polozov, I. V.; Anantharamaiah, G. M.; Segrest, J. P.; Epand, R. P. *Biophys. J.* **2001**, *81*, 949−959.
(17) Lange S.; Nüssler, F.; Kauschke, E.; Lutsch, G.; Cooper, E.; Herrmann, A. *J. Biol. Chem.* **1997**, *272*, 20884−20892.
(18) Abrami, L.; van der Goot, F. G. *J. Cell Biol.* **1999**, *147*, 175−184.
(19) Wang, J. K.; Kiyokawa, E.; Verdin, E.; Trono, D. *Proc. Natl. Acad. Sci. U.S.A.* **2000**, *97*, 394−399.

surface aggregation constant of melittin by about 30% with respect to that of pure POPC LUVs.[4] The minimal surface pressure required to prevent melittin insertion was reported to be practically the same in POPC/SM/chol (1:1:1) and POPC monolayers spread on an aqueous subphase; this suggests that SM does not alter the ability of melittin to partition from the aqueous phase into lipid bilayers.[4] In the ternary POPC/SM/chol mixture, liquid-ordered and liquid-disordered phases coexist.[20,4] Therefore, Gómara et al.[4] suggest that mismatch zones between liquid-ordered and liquid-disordered phases might provide a suitable environment for peptides to self-associate into ion channels. In this respect, we may speculate that the additional dielectric slab revealed by our EIS measurements in outer PC/SM/chol monolayers ($\bar{C}_r$ and $\bar{g}_r$ versus E plots in Figure 7) is due to an accumulation of melittin molecules on top of the liquid-ordered microdomains, where lipid lateral movements are reduced by higher cohesive (packing) properties. These melittin molecules, lying flat on top of the polar heads of the microdomains and possibly partially penetrating them, may form local "carpets" that, intercalated with water molecules, are detected by impedance spectroscopy as a dielectric slab of high conductance. This interpretation would also tentatively explain the disappearance of the features of this additional dielectric slab at the negative applied potentials at which the conductance of the lipid-bilayer moiety undergoes an abrupt increase due to the insertion of the melittin molecules into the bilayer with channel formation. This channel formation taking place at the boundaries of these raftlike microdomains does not contrast with transmembrane peptides having a larger partition coefficient for detergent-soluble fractions of DOPC/SM/chol (1:1:1) vesicles (rich in DOPC) than for detergent-resistant fractions (rich in SM and chol),[20e] as also confirmed by confocal microscopy measurements.[21] In fact, according to this picture, melittin molecules move along on top of the raftlike microdomains but penetrate the lipid bilayer in the mismatch zones around these microdomains.

In conclusion, it has been shown that a biomimetic membrane consisting of a bilayer tethered to mercury via a hydrophilic spacer provides useful information on the effect of the incorporation of the channel-forming peptide melittin in the bilayer by recording impedance spectra over a broad potential range. This is mainly due to the smoothness and fluidity of the liquid-mercury surface. The different substructural elements of the membrane are characterized by different RC meshes in series with each other. In particular, the potential dependence of the circuit element ascribed to the lipid-bilayer moiety, which makes a major contribution to the electrochemical impedance, can be related to the gradual filling of the hydrophilic spacer by the ions moving along the ion channels on the basis of a general approximate approach.

Acknowledgment. We are grateful to Professor W. Knoll and Dr. R. Naumann (Max Planck Institute for Polymer Science, Mainz, Germany) for providing us with the DPTL thiolipid. Thanks are due to to Ente Cassa di Risparmio di Firenze for financial support through the PROMELAB project, to MIUR (Ministry of Education, University and Research) of Italy for financial support through grant PRIN 2003 035241, and to the Ministerio de Ciencia y Tecnologia, proyecto BQU2001-3197, for a fellowship to R.R.L., during whose tenure the present results were obtained.

LA060681X

(20) (a) Samsonov, A. V.; Mihalyov, I.; Cohen, F. S. *Biophys. J.* **2001**, *81*, 1486−1500. (b) Rinia, H. A.; Snel, M. M. E.; van der Eerden, J. P. J. M.; deKruijff, B. *FEBS Lett.* **2001**, *501*, 92−96. (c) Dietrich, C.; Bagatolli, L. A.; Volovyk, Z. N.; Thompson, N. L.; Levi, M.; Jacobson, K.; Gratton, E. *Biophys. J.* **2001**, *80*, 1417−1428. (d) Sáez-Cirión, A.; Nir, S.; Lorizate, M.; Agirre, A.; Cruz, A.; Pérez-Gil, J.; Nieva, J. L. *J. Biol. Chem.* **2002**, *277*, 21776−21785. (e) Gandhavadi. M.; Allende, D.; Vidal, A.; Simon, S. A.; McIntosh, T. J. *Biophys. J.* **2002**, *82*, 1469−1482.

(21) Vidal, A.; McIntosh, T. J. *Biophys. J.* **2005**, *89*, 1102−1108.